



McKay, E., Pruiti, N.G. , Suciu, C., Clerici, M. and Sorel, M. (2024) Alumina Waveguides for Supercontinuum Generation From Near-IR to UV. In: 2024 IEEE Photonics Conference (IPC), Rome, Italy, 10-14 November 2024, pp. 1-2. ISBN 9798350361957 (doi: [10.1109/ipc60965.2024.10799742](https://doi.org/10.1109/ipc60965.2024.10799742))



The University of Glasgow has an agreement with IEEE which allows all University of Glasgow authors to self-archive accepted manuscripts submitted to any of the subscription-based (hybrid) IEEE journals, magazines, or conference proceedings. Authors can immediately self-archive accepted manuscripts in an institutional or subject based repository with a self-attributed CC BY license. The agreement covers all original research and review articles.

Copyright © 2025 IEEE. Reproduced under a [Creative Commons Attribution 4.0 International License](https://creativecommons.org/licenses/by/4.0/).

<https://eprints.gla.ac.uk/345261/>

Deposited on: 27 January 2025

Enlighten – Research publications by members of the University of Glasgow
<https://eprints.gla.ac.uk>

Alumina Waveguides for Supercontinuum Generation From Near-IR to UV

E. McKay¹, N. G. Pruiti¹, C. Suci¹, M. Clerici², M. Sorel^{1,3}

1. School of Engineering, University of Glasgow, Glasgow, United Kingdom

2. Dipartimento di Scienza e Alta Tecnologia, Università degli Studi dell'Insubria, Como, Italy

3. TeCIP, Sant'Anna School of Advanced Studies, Pisa, Italy

Natale.Pruiti@glasgow.ac.uk

Abstract—We develop an ultra-low loss alumina integrated platform for visible light, with sub-dB/cm loss at 450 nm in highly confining waveguides. Using this technology, we generate an octave-spanning supercontinuum in dispersion engineered waveguides, spanning from the near infrared to the ultraviolet spectral regions.

Keywords—alumina, nonlinear, supercontinuum, visible, ultraviolet

I. INTRODUCTION

The generation of novel wavelengths by nonlinear optical processes is at the core of many applications of photonic integrated circuits, such as metrology [1], quantum information processing [2], and spectroscopy [3]. Improving the efficiency of such processes into the deep visible and UV spectral regions would be of substantial benefit, both in terms of increased metrology precision, and in the expansion of these applications into areas that are sensitive to these spectral regions, such as biology and sensing [4].

Despite the availability of a mature large-bandgap photonic platform such as silicon nitride (SiN) [5], accessing nonlinear phenomena at the short-end of the visible spectrum has proved to be a challenge. Even though its transparency window covers the full visible region, SiN shows increasing absorption loss towards the blue end of the spectrum [6].

With a bandgap well below 200 nm [7], Al₂O₃ (alumina) has shown very low loss in the blue and ultra-violet spectral region [8], thus making it a promising candidate for nonlinear optics (NLO) at visible wavelengths. Despite its ultra-wide bandgap, alumina waveguides have found little use in NLO, mainly because of the technological challenges in fabricating the low-loss and thick waveguides required for dispersion engineering. In this work, we designed and fabricated dispersion engineered waveguides from a 700 nm-thick alumina film grown by atomic layer deposition (ALD) [8], and used a 780 nm pump laser to generate supercontinua spanning the near-infrared to the near-ultraviolet.

II. DISPERSION ENGINEERING

Dispersion engineering consists in using the waveguide geometry dispersion to balance that of the material(s), with the aim of controlling the overall group velocity dispersion (GVD). This is a key aspect for NLO, as low GVD values are required

for efficient nonlinear processes. In fact, different processes such as self-phase modulation (SPM), cross-phase modulation (XPM), and optical wave breaking (OWB), rely on temporal and spatial overlap between different pulse components; a condition which is verified only for near-zero values of the GVD [9].

Since amorphous alumina has a relatively low refractive index (1.64 at 780 nm) [8], relatively thick films are required for near-zero GVD. Finite difference eigenmode (FDE) simulations based on ellipsometric data, show that a film thickness of 700 nm provides low GVD at a pump wavelength of 780 nm, provided the waveguides are left unclad, as show in Fig. 1. In fact, GVD is strongly normal if an upper cladding is used for both TE and TM pumps.

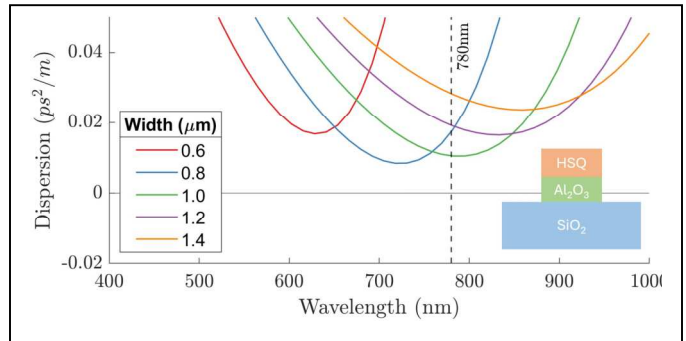


Fig. 1. Simulated dispersion of TE₀₀ mode in 700 nm-thick alumina waveguides with 100 nm residual HSQ mask. Inset shows schematic of waveguide cross-section.

III. WAVEGUIDE FABRICATION

For this work, we designed and fabricated 700 nm-thick alumina waveguides ranging from 700 nm to 1400 nm in width. The alumina film was deposited by oxygen plasma enhanced ALD, which provides higher deposition rate compared to the more standard thermal process [8]. We defined waveguides using and HSQ mask patterned through e-beam lithography, and transferred the pattern to the alumina core using a BCl₃-based etching process [8]. The residual mask, with an approximated thickness of 100 nm, was left on the waveguide, that were left unclad to achieve the desired low GVD value. The chip was manually cleaved to expose waveguide facets for end-fire coupling, leaving 12-mm-long waveguides.

IV. SUPERCONTINUUM GENERATION

We employed a Menlo Systems C-Fiber 98 780 High Power laser with a 90 fs pulse width and a measured maximum pulse energy of 1.6 nJ for the generation of the supercontinuum. Pulse polarisation and power were controlled by a pair of half-wave plate and polarisation beam splitter, and the beam was coupled in and out of the chip using aspheric lenses with typical insertion loss of ~ 11 dB. The output beam was finally focused on a lensed fibre attached to an OceanOptics HR2000+ spectrometer with a wavelength range of 200 nm to 1100 nm.

We observed considerably more spectral broadening for TE-polarised light than TM-polarised light, in line with predictions based on GVD simulations. While substantial broadening was produced in all fabricated waveguides, in those with widths spanning from 700 to 1100 nm, emission of a dispersive wave is observed at blue wavelengths. To explain the mechanisms underlining the generation of supercontinua, we used the generalised nonlinear Schrodinger equation (GNLSE) to simulate pulse evolution during propagation through 12 mm long waveguides. A simulation of the spectral evolution in an 800-nm-wide waveguide is shown in Fig. 2.A: initially, significant symmetrical broadening occurs through self-phase-modulation (SPM). After sufficient broadening has taken place, optical-wave breaking (OWB) triggers the emission of a dispersive wave (DW) at the blue end of the spectrum. This behaviour is reflected as well by the output spectrum measured at different input power levels, illustrated in Fig. 2.B: at low power levels, only a symmetric spectral broadening is observed, while formation of dispersive wave in the blue is observed for input powers greater than 100 mW.

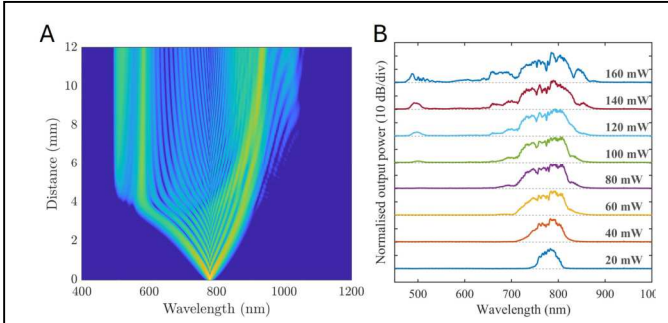


Fig. 2. (A) Simulated spectral evolution in 800 nm-wide waveguide pumped at 780 nm as function of propagation distance. (B) Measured output spectra in a 800 nm-wide waveguide as function of pump power, with each baseline shifted by 20 dB.

The broadest spectrum, with a -40 dB band spanning from 382 nm to 952 nm, was obtained by coupling a mixture a 5:2 ratio of TM to TE light into an 800 nm-wide waveguide, as illustrated in Fig. 3.

In conclusion, by developing low-loss and dispersion-engineered alumina waveguides, we have demonstrated the generation of super-continuum from ~ 380 nm to ~ 950 nm at a level of -40dB. This results is of great relevance to the exploitation of waveguide non-linearities in the visible and UV spectral regions.

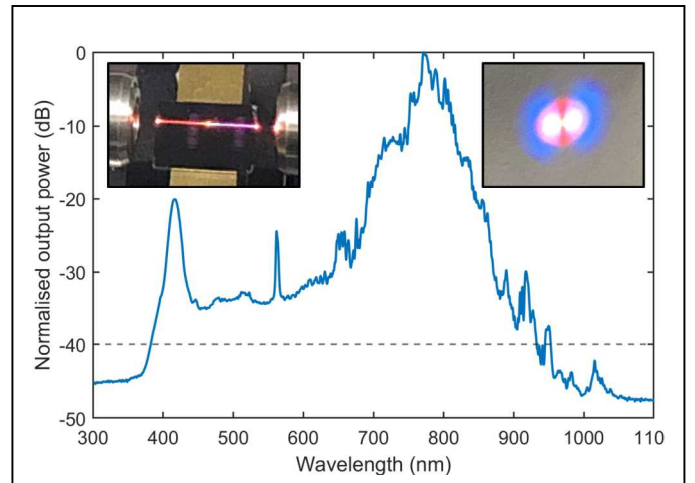


Fig. 3. Measured supercontinuum in 12 mm-long, 800 nm-wide alumina waveguide, with average pump power of 160 mW. The polarisation of the input light is 5:2 TM:TE. Inset photographs shows the scattered light from the waveguide (left) and a far-field output spot (right).

ACKNOWLEDGMENT

We would like to thank the staff of the James Watt Nanofabrication Centre, particularly James Grant, for providing support for the process development work required to produce the waveguide devices. We also acknowledge the National Physical Laboratory (NPL), Defence Science and Technology Laboratory (DSTL) and EPSRC for funding.

REFERENCES

- [1] Z. L. Newman, V. Maurice, T. Drake, et al., "Architecture for the photonic 244 integration of an optical atomic clock," *Optica* 6, 680–685 (2019).
- [2] Wang, J., Sciarrino, F., Laing, A. et al. "Integrated photonic quantum technologies," *Nat. Photonics* 14, 273–284 (2020)
- [3] R. Antoine and P. Dugourd, "UV-Visible Absorption Spectroscopy 248 of Protein Ions," in *Photophysics of Ionic Biochromophores*, 249 S. Brondsted Nielsen and J. A. Wyrer, eds. (Springer, Berlin, Heidelberg, 250 2013), *Physical Chemistry in Action*, pp. 141–153
- [4] X. Shu, L. J. Beckmann, and H. F. Zhang, "Visible-light optical coherence tomography: a review," *J. Biomed. Opt.* 22, 121707 (2017)
- [5] Martin H. P. Pfeiffer, Clemens Herkommer, Junqiu Liu, Hairun Guo, Maxim Karpov, Erwan Lucas, Michael Zervas, and Tobias J. Kippenberg, "Octave-spanning dissipative Kerr soliton frequency combs in Si_3N_4 microresonators," *Optica* 4, 684–691 (2017)
- [6] Mateus Corato-Zanarella, Xingchen Ji, Aseema Mohanty, and Michal Lipson, "Absorption and scattering limits of silicon nitride integrated photonics in the visible spectrum," *Opt. Express* 32, 5718–5728 (2024)
- [7] Elena O. Filatova and Aleksei S. Konashuk, "Interpretation of the Changing the Band Gap of Al_2O_3 Depending on Its Crystalline Form: Connection with Different Local Symmetries," *The Journal of Physical Chemistry C* 2015 119 (35), 20755–20761
- [8] E. McKay, N. G. Pruiti, S. May, and M. Sorel, "High-confinement alumina waveguides with sub-dB/cm propagation losses at 450 nm," *Sci. Reports* 13, 19917 (2023)
- [9] L. Zhang, Q. Lin, Y. Yue, et al., "Silicon waveguide with four zero-dispersion wavelengths and its application in on-chip octave-spanning supercontinuum generation," *Opt. Express* 20, 1685–1690 (2012)